

## Gradient-based Optimization of Parameterized CAD Geometries

Timothée Leblond<sup>1,2</sup>, Pierre Froment<sup>1</sup>, Paul de Nazelle<sup>1</sup>, Reda Sellakh<sup>2</sup>, Philippe Serré<sup>2</sup>, Gaël Chevallier<sup>3</sup>

<sup>1</sup> Technological Research Institute SYSTEMX, F-91120 Palaiseau, France,  
{timothee.leblond,pierre.froment,paul.denazelle}@irt-systemx.fr

<sup>2</sup> LISMMA – EA-2336, Supméca, F-93407 Saint-Ouen, France,  
{reda.sellakh,philippe.serre}@supmeca.fr

<sup>3</sup> FEMTO-ST Institute – UMR 6174, CNRS-UFC-ENSMM-UTBM, F-25000 Besançon, France,  
gael.chevallier@univ-fcomte.fr

### 1. Abstract

This paper presents a novative method for gradient-based optimization with regard to CAD parameters. This method allows to respect manufacturing, design and surface quality rules, particularly required in computational fluid dynamics (CFD). It can be used with any objective function available in adjoint solvers (both in structural and CFD). To prove the efficiency of the method, the workflow schedule was apply on an air-conditionning duct so as to maximize the eigen frequency and then to minimize the pressure drop.

**2. Keywords:** CAD parameters, sensitivity, optimization, CFD, adjoint solvers.

### 3. Introduction

Thanks to HPC, numerical optimization methods are more and more used to determine an optimal shape at a lower cost in faster.

Among these methods, both design of experiments and surrogate modeling methods allow to work directly on CAD parameters with the exception that the design space, i.e. the number of parameters, should be confined enough in order to be explored within a reasonable computational time. Other methods are based on the gradients provided by adjoint solvers, that is to say on the sensitivity of a cost function with respect to the displacement boundaries. The sensitivity is used to know how to change the shape at any node of the mesh to obtain better performance. They naturally get over the number of degrees of freedom but they are computed with respect to the coordinates of the vertices of the surface mesh. However, since manufacturing constraints are difficult to express mathematically, they are not taken into account during the mesh morphing. This drawback can be avoid by using a CAD model that implicitly includes these manufacturing constraints.

To take advantage of both approaches, this method proposes to extend these gradients to CAD parameters. This paper presents the developments of this method and its integration into an optimization loop. Applications on structural and CFD problems will be presented to prove the feasibility of this approach and the possible gains about the number of resolutions.

### 4. Shape Sensitivity with regard to CAD Parameters

During an optimization, the shape of the geometry is modified in order to improve its performance regarding an objective function. Here, it can only be modified thanks to CAD parameters. So, it is necessary to determine the shape sensitivity of the objective function with regard to CAD parameters ( $d_{\alpha}J$ ) given by Eq.(1).

$$d_{\alpha}J = \partial_x J \times \partial_{\alpha} x \quad (1)$$

$\partial_x J$  represents the shape sensitivity of the objective function  $J$  with regard to node displacements. It is given by adjoint solvers and indicates how to move the nodes of the mesh to improve the objective function. In that scheme, any objective function available in adjoint solvers can be applied in this equation. The term  $\partial_{\alpha} x$  represents the shape sensitivity with regard to CAD parameters and indicates how the shape is impacted by a CAD parameter perturbation.

#### 4.1. State of the Art

The bibliography have pesented three ways to compute the sensitivity of the shape with regard to CAD parameters. The first one is an analytic way that suggests to derivate the CAD surface equations. Yu et al. [10] present the main advantage of this method, i.e. the accuracy of the results. However, it is necessary to know the explicite definition of the shape in order to derivate these equations. Mostly, these formal expressions are not available in the CAD

systems that are often proprietary software and that use implicate geometric solvers. It is therefore difficult to compute shape derivation.

The numerical approach consists in evaluating the gradient by finite differences as proposed by Armstrong et al. [1]. It compares the initial and perturbed geometries prior to generate the meshes. This approach requires the disponibility of the geometric representation of CAD models [3] so as to be able to work with  $u, v$  coordinates. Moreover, a parameter variation may result in additionnal patches and different naming [4]. These changes makes surface identification difficult [6].

Another numerical approach is based on the discretization of the CAD geometry. The evaluation of the gradient is done by finite differences between both the meshes of the initial shape and the perturbed shape. The main difficulty is to determine the deformation field that projects one mesh on the other and that limits the distortion of cells. The deformation of the initial mesh is presented in many methods and Toivanen et al. [9] present one of them but the cell distortion is hardly mastered. Robinson et al. [6] propose to project the nodes of the initial mesh on the deformed one along the normal but it causes difficulties on the process and requires adjustments.

#### 4.2. Proposed Method

When meshes are used to compute the gradient, one of the main problems is the absence of isoconnectivity between both the mesh of the initial shape and the mesh of the geometry after the variation of a parameter. The evaluation of the displacement of any node of the mesh is used to compute the sensitivity. To determine this displacement, the mesh of the initial shape is morphed on the mesh of the perturbed shape. During this operation, it is easy to follow each node and create an isoconnectivity between the mesh of both geometries. The harmonic projection [2, 5] is used to project 3D geometries on a 2D parametric domain, it corresponds to a reparameterization in 2D space. The latter is considered as a reference space for both shapes.

The theoretical process is detailed with a geometry  $\Omega_\alpha$  with one frontier. At each iteration of the optimization,  $\alpha_0$  represents the set of CAD parameters for the initial shape  $\Omega_{\alpha_0}$ , considered as the reference geometry. The perturbed geometry  $\Omega_{\alpha_i}$  is obtained after the variation of  $i^{\text{th}}$  parameter. The respective meshes of the initial and the perturbed shapes are noted  $\tilde{\Omega}_{\alpha_0}$  and  $\tilde{\Omega}_{\alpha_i}$ .

Each mesh is projected by a harmonic transformation on a unit disk, respectively noted  $\tilde{\mathcal{D}}_{\alpha_0}$  and  $\tilde{\mathcal{D}}_{\alpha_i}$ . Given  $\mathcal{U}_{\alpha_0}$  and  $\mathcal{U}_{\alpha_i}$  the functions used to obtain respectively these disks and  $\mathcal{U}_{\alpha_0}^{-1}$  and  $\mathcal{U}_{\alpha_i}^{-1}$  the inverse functions:

$$\begin{aligned} \mathcal{U}_\chi : \tilde{\Omega}_\chi \subset \mathbb{R}^3 &\longrightarrow \tilde{\mathcal{D}}_\chi(0, 1) \\ (x, y, z) &\longmapsto \begin{cases} u_\chi(x, y, z) \\ v_\chi(x, y, z) \end{cases} \quad \chi \in \{\alpha_0, \alpha_1, \dots, \alpha_i, \dots, \alpha_p\} \end{aligned} \quad (2)$$

The figure 1 gives an illustration of the previous step. For example, a cube, opened on the lower face, is considered as the reference shape  $\Omega_{\alpha_0}$ . The variation of the parameter controlling the height of an edge provides the perturbed shape  $\Omega_{\alpha_i}$ . The respective meshes  $\tilde{\Omega}_{\alpha_0}$  and  $\tilde{\Omega}_{\alpha_i}$ , done separately, are projected onto the disks  $\tilde{\mathcal{D}}_{\alpha_0}$  and  $\tilde{\mathcal{D}}_{\alpha_i}$ .

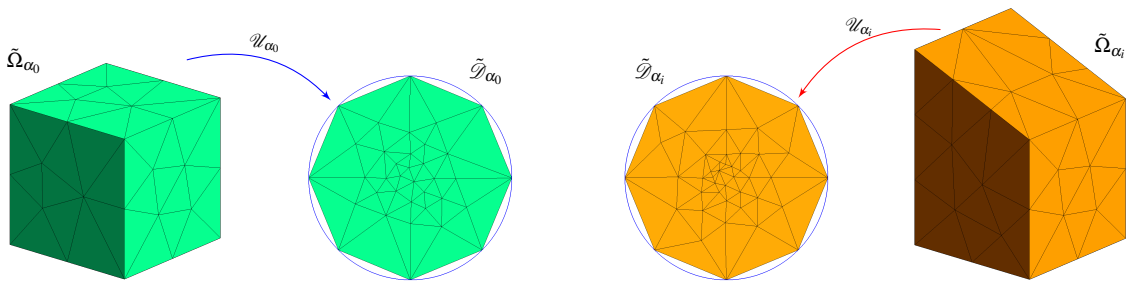


Figure 1: Projection of the mesh of the initial and perturbed shapes

The harmonic function is one-to-one, so it is possible to apply  $\mathcal{U}_{\alpha_i}^{-1}$  on the disk  $\tilde{\mathcal{D}}_{\alpha_0}$ . The nodes of  $\tilde{\mathcal{D}}_{\alpha_0}$  are interpolated with ones of  $\tilde{\mathcal{D}}_{\alpha_i}$ . So, the initial mesh  $\tilde{\Omega}_{\alpha_0}$  is fitted on the perturbed mesh  $\tilde{\Omega}_{\alpha_i}$ . Thus, the new values of the coordinates of  $\tilde{\Omega}_{\alpha_0}$  are known. The evaluation of the perturbation is given by the finite differences of the old and new coordinates of each node, as given by Eq.(3).

$$\partial_{\alpha_i} \Omega \simeq \frac{\mathcal{U}_{\alpha_i}^{-1}(\tilde{\mathcal{D}}_{\alpha_0}(0, 1)) - \tilde{\Omega}_{\alpha_0}}{\delta \alpha_i} \quad i = 1 \dots p \quad (3)$$

It is now possible to compute the Eq.(1). Nevertheless, the presented method requires that the 3D surface and the parametric domain are homeomorphic. In this paper, we handle CAD geometries so has to make them be home-

omorphous to a disk  $\tilde{\mathcal{D}}_\chi$ . Indeed, the surface is cut to obtain a homeomorphic surface to a disk. This solution was used to verify the feasibility of the proposed approach in an optimization loop.

### 5. Applications in structure and CFD

The optimization loop uses the result of the Eq.(1) into a gradient descent algorithm. The optimization loop can be used in structural and CFD domains. In direct optimization, even if the computation time is limited, it is possible with the gradient to directly improve the solution, particularly in CFD where the computational cost can be very expensive. This method, breaking away from the usual industrial process, was applied on different academic test cases. Two of them are detailed after and a summary of specific ones is done in the table 1.

As presented by the figure 2, the initial values of the parameters  $\alpha_0$  are given to the CAD software. The outputs are the initial geometry  $\Omega_{\alpha_0}$  and every geometries  $\Omega_{\alpha_i}$  corresponding to the variation of each parameter  $\alpha_i$ . In this case, the variation of each parameters are chosen arbitrarily at 5% of the initial value. All these geometries are meshed and the mesh of the initial one is given directly to the primary and the adjoint solvers. During the resolution, every meshes, corresponding to each perturbed geometries, are compared to the initial mesh by the processus presented in 4.2. Both information given by the adjoint solver and the sensitivity computation is used in an optimizer to determine the new values of  $\alpha_0$  for the next iterations.

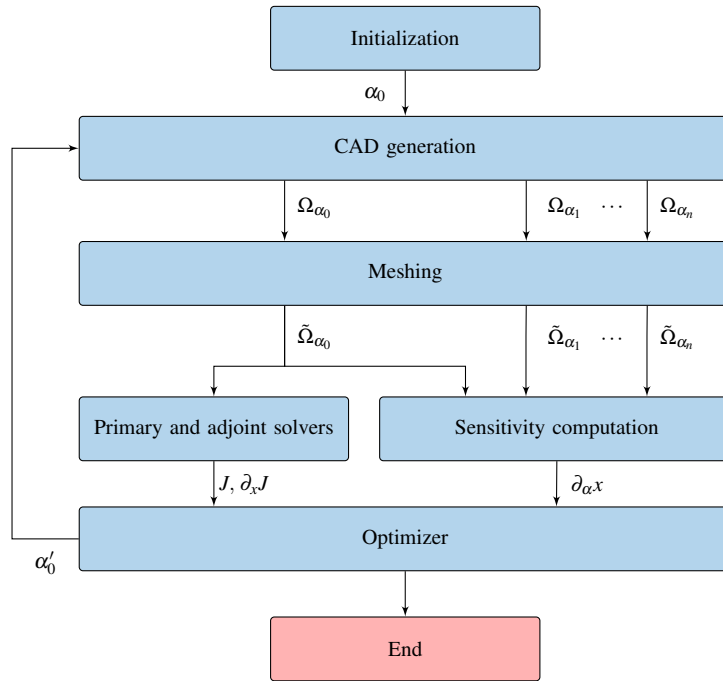


Figure 2: Scheme of the optimization loop

First, gradients from Nastran (available since 1995) were used to prove the efficiency of the method. The optimization problem was to maximize the eigen frequency of an air-conditionning duct. The CAD geometry (figure 3(a)) is a multi-section surface defined by 7 sections. The parameters and the boundary conditions, applied to the first and the last section, give 13 parameters and a frequency of 300 Hz. After about 40 iterations, the frequency was more than 1000 Hz. So, the optimization improve significantly the shape regarding this objective function only by modifying CAD parameters.

Second, the optimization problem was to minimize the pressure drop of the air-conditionning duct. The Star-CCM+ adjoint solver was used to compute the sensitivity of the objective function. The CAD geometry (figure 3(b)) has a S-bend profile defined by a multi-section surface with 7 sections. The parameters of each section and the boundary conditions give a model with 25 parameters and an initial pressure drop of 530 Pa. After 14 iterations, the gain was around 40 percent only by modifying CAD parameters.

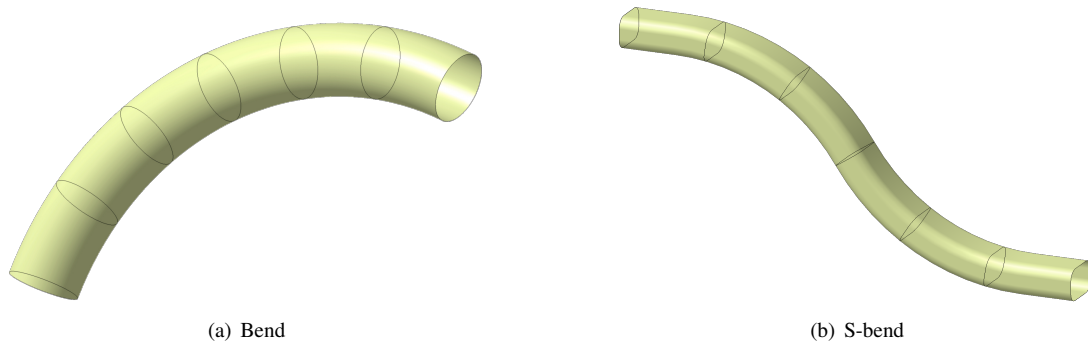


Figure 3: CAD geometries used in optimization loops

Table 1: Summary of results obtained with the optimization loop in structure and CFD – *Structure<sup>1</sup>*: maximizing the eigen frequency – *Structure<sup>2</sup>*: minimizing this displacement due to a force – *CFD*: minimizing the pressure drop

| Physic involved        | Profile of duct | Number of parameters | Number of iterations | Objective function |           | Gain [%] |
|------------------------|-----------------|----------------------|----------------------|--------------------|-----------|----------|
|                        |                 |                      |                      | initial            | final     |          |
| Structure <sup>1</sup> | Bend            | 13                   | 36                   | 306.2 Hz           | 1007.6 Hz | 229      |
| Structure <sup>1</sup> | Bend            | 14                   | 52                   | 217.6 Hz           | 673.9 Hz  | 210      |
| Structure <sup>2</sup> | Bend            | 11                   | 45                   | 9.05 mm            | 1.21 mm   | 86.6     |
| Structure <sup>2</sup> | Bend            | 30                   | 66                   | 5.68 mm            | 0.55 mm   | 90.3     |
| CFD                    | Bend            | 10                   | 23                   | 4.86 Pa            | 2.44 Pa   | 49.8     |
| CFD                    | Bend            | 25                   | 15                   | 4.32 Pa            | 1.75 Pa   | 59.5     |
| CFD                    | S-bend          | 25                   | 14                   | 532 Pa             | 302 Pa    | 43.2     |

## 6. Conclusion

Current results are obtained by cutting the CAD geometries in order to make the 3D surface be homeomorphic to a disk. However, this requires an extra step to the designer to find a cutting surface valid whatever the value of parameters. Further developments will avoid this extra step and project multi-boundary surface on the disk.

Results prove the feasibility of the presented method with significant gain regarding the number of resolutions. It would be interesting to use these gradients in more complex algorithms such as conjugate gradient or quasi-Newton or in response surface modeling.

In this paper, structural and CFD domains are separately treated. Further developments will allow to apply this loop on multiphysic cases.

## 7. Acknowledgements

This research work has been carried out under the leadership of the Technological Research Institute SystemX, and therefore granted with public funds within the scope of the French Program "Investissements d'Avenir".

We thank CD-Adapco France for providing us the Star-CCM+ licenses.

## 8. References

- [1] C.G. Armstrong, T.T. Robinson, H. Ou and C. Othmer. *Linking adjoint sensitivity maps with CAD parameters*, Evolutionary methods for design, optimization and control, pages 234-239, 2007.
- [2] X.D. Gu and S.T. Yau. *Computational conformal geometry*, volume 3 of Advanced lectures in mathematics, International Press, 2008.
- [3] E. Hardee, K.H. Chang, J. Tu, K.K. Choi, I. Grindeanu and X. Yu. *A CAD-based design parameterization for shape optimization of elastic solids*, Advances in Engineering Software, vol. 30, no. 3, pages 185-199, 1999.

- [4] J. Kripac. *A mechanism for persistently naming topological entities in history-based parametric solid models*, Computer-Aided Design, vol. 29, no. 2, pages 113-122, 1997.
- [5] J.F. Remacle, C. Geuzaine, G. Compère and E. Marchandise. *High-quality surface remeshing using harmonic maps*, International Journal for Numerical Methods in Engineering, vol. 83, pages 403-425, 2010.
- [6] T.T. Robinson, C.G. Armstrong, H.S. Chua, C. Othmer and T. Grahs. *Sensitivity-based optimization of parameterized CAD geometries*, In Proceedings of 8th World Congress on Structural and Multidisciplinary Optimization. ISSMO, 2009.
- [7] T.T. Robinson, C.G. Armstrong, H.S. Chua, C. Othmer and T. Grahs. *Optimizing parameterized CAD geometries using sensitivities-based on adjoint functions*, Computer-Aided Design and Applications, pages 253-268, 2012.
- [8] D. Thévenin and G. Janiga. *Optimization and computational fluid dynamics*, Springer, 2008.
- [9] J.I. Toivanen and J. Martikainen. *A new method for creating sparse design velocity fields*, Computer Methods in Applied Mechanics and Engineering, vol. 196, no. 1-3, pages 528-537, 2006.
- [10] G. Yu, J.D. Müller, D. Jones and F. Christakopoulos. *CAD-based shape optimisation using adjoint sensitivities*, Computers & Fluids, vol. 46, no. 1, pages 512-516, 2011. 10th ICFD Conference Series on Numerical Methods for Fluid Dynamics.